Journal of Alloys and Compounds 499 (2010) 212–214

Contents lists available at ScienceDirect

Journal of Alloys and Compounds

journal homepage: www.elsevier.com/locate/jallcom

The effect of B site doping on infrared emissivity of lanthanum manganites $La_{0.8}Sr_{0.2}Mn_{1-x}B_xO_3$ (B = Ti or Cu)

Xingmei Shen*, Guoyue Xu, Chunming Shao

College of Material Science & Engineering, Nanjing University of Aeronautics and Astronautics, Yu Dao Street 29, Nanjing 210016, China

ARTICLE INFO

Article history:
Received 11 December 2009
Received in revised form 18 March 2010
Accepted 18 March 2010
Available online 25 March 2010

Keywords:
Ceramics
Solid-state reaction
Optical properties
Light absorption and reflection

ABSTRACT

The lanthanum manganites $La_{0.8}Sr_{0.2}Mn_{1-x}B_xO_3$ (B = Ti or Cu, $0 \le x \le 0.4$) were prepared by standard solid-state reaction method. The structure, infrared absorption, electron spin resonance (ESR) and infrared normal emissivity (ε_N) in the 8–14 μm waveband of the samples were systematically investigated. The samples are perovskite with distorted rhombohedral structure. Compared to $x = 0$ sample with ε_N value 0.693, infrared absorption occurred in the 8–14 μm waveband leads to high emissivity value of the B site doping samples ($\varepsilon_{Ti} = 0.912$ and $\varepsilon_{Cu} = 0.894$), and the ε_N decreases slightly with increasing doping level due to decreasing transition probability indicated by ESR results. The ε_N changes slightly in the temperature range 293–373 K, from 0.9 to 0.882 for Ti doping and from 0.886 to 0.879 for Cu doping, owing to the weakening of the double-exchange interaction between Mn^{3+} and Mn^{4+}.

1. Introduction

The ABO_3-type lanthanum manganites have attracted much attention owing to their interesting physical properties, e.g. CMR effect. As La in A site is partially replaced by Sr, the sample undergoes metal–insulator (MI) phase transition [1–4]. The above mentioned phenomenon has been explained by means of double-exchange interaction between Mn^{3+} and Mn^{4+}, and electron–phonon interaction relating to Jahn–Teller-type lattice distortion of the MnO_6 octahedra [5–8]. In general, infrared emissivity of metal is low, while that of insulator is high. Thus, the infrared emissivity of Sr doped sample changes significantly with temperature, which make them attractive as thermal control material [9–11]. Since the Mn^{3+}–O–Mn^{4+} network plays an important role in physical properties, several studies on doping at Mn site have been undertaken during the past few years. Aslibeiki et al. have reported that the substitution of Mn by Ti ($0 \le x \le 0.075$) in $La_{0.8}Sr_{0.2}Mn_{1-x}Ti_xO_3$ compound decreases the MI transition temperatures and system becomes an insulator, which can be explained by the percolation model, and the reentrant spin glass state accompanied by the FM transition exists in high doped samples [12]. The magnetic properties and low-field magnetoresistance of $La_{0.7}Sr_{0.3}Mn_{0.9}Cu_{0.1}O_3$ compounds have been studied by Zhao et al., and the Mn-site substitution by various M could not enhance the MR response at a low magnetic field of 2 kOe [13]. Kallel et al. have reported that the substitution of 50% Mn with Ti changes the structure of $La_{0.5}Sr_{0.5}Mn_{0.5}Ti_{0.5}O_3$ compound from the tetragonal to rhombohedral symmetry and cuts-off the long-range ordering of Mn^{3+}/Mn^{4+}, hence, the localization of e_g electrons is suppressed and the CO is drastically destroyed by the doping [14]. Castellano et al. have reported that the Cu substitution weakens in a relevant and outstanding way the FM long-range phase in the $(La_{1-x}Ca_x)(Mn_{1-y}Cu_y)O_3$ compound with $x < 0.50$ while the CO phase in the second class of samples ($x > 0.50$) results to be only slightly conditioned [15]. And the substitutions of other metal ions for Mn have also been studied [16–18]. Then, what about the infrared emissivity of B site doped manganites? However, studies on the effect of B site doping on infrared emissivity of lanthanum manganites have not been reported yet. In this work, we investigated the structure, infrared absorption, electron spin resonance and infrared normal emissivity (ε_N) in the 8–14 μm waveband of B site doped lanthanum manganites $La_{0.8}Sr_{0.2}Mn_{1-x}B_xO_3$ (B = Ti or Cu).

2. Experimental procedures

A series of B site doped lanthanum manganites $La_{0.8}Sr_{0.2}Mn_{1-x}B_xO_3$ (B = Ti or Cu, $x = 0$, 0.1, 0.2, 0.3 and 0.4) were prepared by standard solid-state reaction method. La_2O_3, $SrCO_3$, TiO_2, CuO and MnO_2 were used as raw materials and La_2O_3 was fired in air at 1173 K for 7 h before use. Ethanol was added as a milling medium together with the raw materials. After milling for 12 h, the mixture was air-dried at 353 K to remove the ethanol and calcined at 1273 K, and then pressed into discs with polyvinyl alcohol. The samples were finally sintered at 1473 K for 24 h.

The structure of the samples was characterized by Bruker D8 X-ray powder diffraction (XRD) using Cu Kα radiation ($\lambda = 0.15405$ nm) operated at 40 kV and 40 mA. Infrared absorption (IR) spectra were measured by NEXUS-670 Fourier transform infrared spectrophotometer. Electron spin resonance (ESR) measurements

* Corresponding author. Tel.: +86 25 84892903; fax: +86 25 84892951.
E-mail address: xxxxmx@126.com (X. Shen).

0925-8388/$ – see front matter © 2010 Elsevier B.V. All rights reserved.
doi:10.1016/j.jallcom.2010.03.169

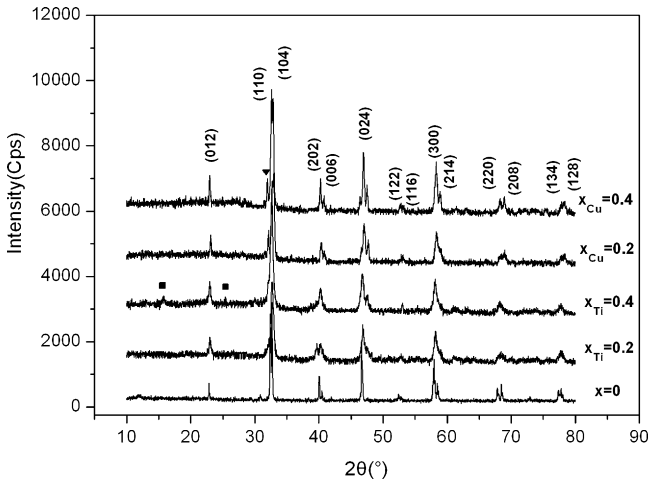

Fig. 1. X-ray diffraction patterns of Ti and Cu doped samples ($x = 0$, 0.2 and 0.4). ■, ▼ indicate additional peaks in Ti and Cu doped samples, respectively.

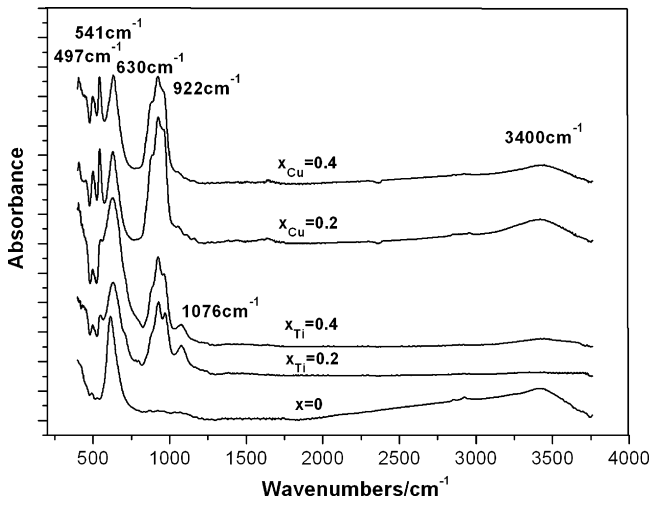

Fig. 2. Infrared absorption spectra of Ti and Cu doped samples with different doping levels.

were performed at 9.236 GHz with the JES-FEIXG spectrometer using a microwave power of 0.4 mW and modulation amplitude of 3.2 G. The infrared normal emissivity (ε_N) was measured by the IR-2 infrared emissometer in the 8–14 μm waveband.

3. Results and discussion

Fig. 1 shows the XRD patterns of Ti and Cu doped samples ($x = 0$, 0.2 and 0.4), respectively. As can be seen from the figure, all of the samples exhibit the characteristic peaks of the perovskite structure. For $La_{0.8}Sr_{0.2}MnO_3$ (LSMO, $x = 0$) sample, a single perovskite phase was detected and the separation of peaks at $2\theta \approx 32.6^\circ$, 40.3°, 58.3° and 68.4° indicates that the sample is distorted rhombohedral with space group R-3c ($a = 0.5518$ nm, $c = 1.3351$ nm, JCPDS Card, No. 53-0058). For $La_{0.8}Sr_{0.2}Mn_{1-x}Ti_xO_3$ samples ($a = 0.5557$ nm and $c = 1.3305$ nm for $x = 0.2$, $a = 0.5565$ nm and $c = 1.3284$ nm for $x = 0.4$), the twin peaks of rhombohedral perovskite (3 0 0)–(2 1 4) at $2\theta \approx 58^\circ$ and (2 2 0)–(2 0 8) at $2\theta \approx 68^\circ$ coalesced into single peaks. This indicates that the perovskite lattice tends to a higher symmetry as Ti doped level x increases. When the dopant is 0.4, two weak peaks were detected in addition to those of rhombohedral perovskite. For Cu doped samples ($a = 0.5559$ nm and $c = 1.3152$ nm for $x = 0.2$, $a = 0.5592$ nm and $c = 1.3300$ nm for $x = 0.4$), one weak additional peak was also detected for $x = 0.4$ sample. The presence of these weak additional peaks indicates the complex order of the perovskite. In general, ordering lowers the symmetry, consequently, the diffraction patterns have more peaks due to the fewer systematic absences. Thus, the order transformation of a crystal structure can frequently be detected by observing the appearance of the superlattice reflections of the ordered structure additionally to the fundamental reflection of that superlattice [19]. Therefore, a single-phase of ordered structure for $x = 0.4$ sample was formed.

Fig. 2 shows the infrared absorption spectra of Ti and Cu doped samples with different doping levels. From the figure, it can be seen that a single peak appears around 630 cm^{-1} for $x = 0$ sample, which can be attributed to the internal stretching motion of the Mn ion against the oxygen in MnO_6 octahedron. Usually, there are three phonon modes in perovskite. The external mode, located around 170 cm^{-1}, represents a vibrating motion of the La ions against the MnO_6 octahedra. The bending mode, located near 330 cm^{-1}, reflects an internal motion of Mn–O–Mn bond. The stretching mode, located around 600 cm^{-1}, corresponds to an internal motion of Mn–O bond [20,21]. For Ti doped samples, new peaks occurred at 497 cm^{-1}, 922 cm^{-1} and 1076 cm^{-1} in addition to 630 cm^{-1}. The slighter separation of peaks around 630 cm^{-1} and 922 cm^{-1} for $x = 0.4$ sample than that for $x = 0.2$ sample indicates a higher symmetry of the structure. This is consistent with the XRD results shown in Fig. 1. For Cu doped samples, the intense peaks occurred at 497 cm^{-1} and 541 cm^{-1} may be due to the asymmetric vibration in distorted crystal lattice. The broad absorption peak appearing around 3400 cm^{-1} in the samples is a characteristic of absorbed water.

Electron spin resonance (ESR) spectra of $La_{0.8}Sr_{0.2}Mn_{1-x}Ti_xO_3$, $La_{0.8}Sr_{0.2}Mn_{1-x}Cu_xO_3$ and $La_{0.8}Sr_{0.2}MnO_3$ samples are shown in Fig. 3. As can be seen in the figure, Ti and Cu doped samples show paramagnetic (PM) signals and LSMO sample ($x = 0$) is in the ferromagnetic (FM) state. The intensity and width of the paramagnetic line of $x = 0.2$ for Ti and Cu doped samples are larger than those of $x = 0.4$ samples. The intensity results indicate that the concentration of single electron for $x = 0.4$ sample is lower than that for $x = 0.2$ sample, and intensity of Ti doped samples is higher than that of Cu doped samples. With the doping level increasing ($x = 0.4$), the perovskite lattice tends to a higher symmetry for Ti doped samples. On the other hand, ordered structure leads to larger lattice distortion (shown in Fig. 1), which results in the enhancement of spin-lattice relaxation. Then, the extension of relaxation time results in the narrowing of the linewidth.

Fig. 4 shows the relationship between infrared normal emissivity (ε_N) in the 8–14 μm waveband and doping level (x) with

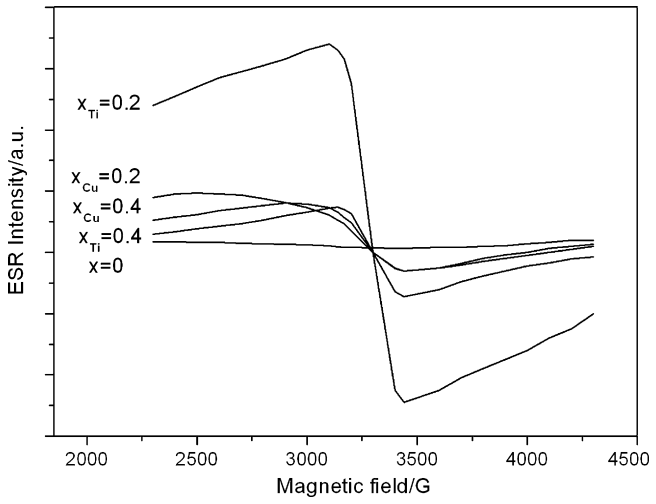

Fig. 3. Electron spin resonance spectra of Ti and Cu doped samples.

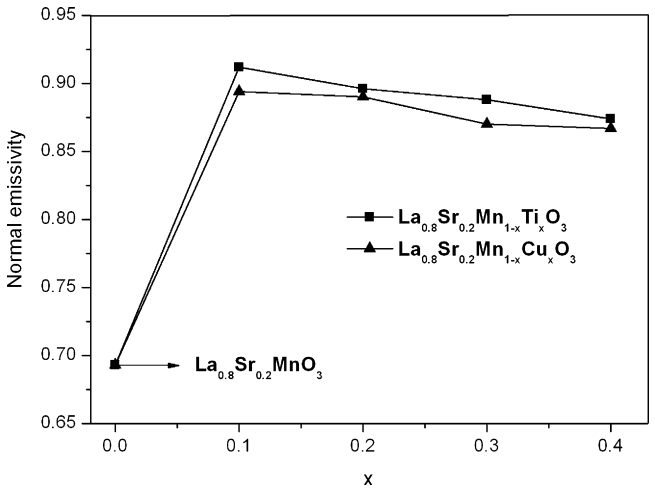

Fig. 4. The relationship between infrared normal emissivity (ε_N) in the 8–14 μm waveband and doping level (x) with different doping ions.

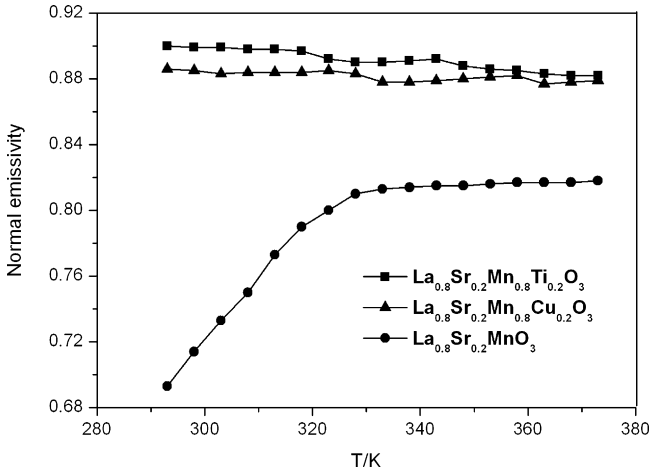

Fig. 5. The temperature dependence of the ε_N of $x = 0$ and 0.2 samples in the temperature range of 293–373 K.

different doping ions. From the figure, it can be seen that the ε_N of LSMO ($x = 0$) is 0.693. As B site is doped ($x = 0.1$), the ε_N increases drastically, from 0.693 to 0.912 for Ti doped sample and from 0.693 to 0.894 for Cu doped sample. According to Kirchhoff law concerning the equality of the emissivity and absorptivity, this may be attributed to the strong absorption peaks in the 8–14 μm waveband appearing around 10.8 μm (922 cm^{-1}), as shown in Fig. 2. For LSMO, no infrared absorption occurs in the 8–14 μm waveband. However, the ε_N decreases slowly with increasing doping level. The infrared reflectance results reported by Shimazaki in the 8–14 μm waveband indicate that free electrons increase with increasing doping level, and the increased mobility of free electrons results in the decrease of ε_N [9]. Furthermore, the electronic orbit transition can result in high ε_N value. According to Fig. 3, the concentration of single electron decreases with increasing doping level, indicating decreasing transition probability. Therefore, the ε_N decreases with increasing doping level. This is also the reason for higher ε_N value of Ti doped samples.

Fig. 5 shows the temperature dependence of the ε_N of $La_{0.8}Sr_{0.2}Mn_{0.8}Ti_{0.2}O_3$, $La_{0.8}Sr_{0.2}Mn_{0.8}Cu_{0.2}O_3$ and $La_{0.8}Sr_{0.2}MnO_3$ samples in the temperature range of 293–373 K. As can be seen from the figure, the ε_N of LSMO increases with increasing temperature and changes significantly in the temperature range 293–328 K, from 0.693 to 0.818, due to the metal–insulator transition [11]. However, for Ti and Cu doped samples, the ε_N changes slightly in the whole temperature range, from 0.9 to 0.882 and from 0.886 to 0.879, respectively. This may be related to the weakening of the double-exchange interaction between Mn^{3+} and Mn^{4+}. As B site is doped by Ti or Cu ions, Mn ions are partially replaced by Ti^{4+} or Cu^{2+}. The Cu ions exist in Cu^{3+} form with low Cu doping ($x \leq 0.05$) and in Cu^{2+} form with $x = 0.2$ doping [22]. Then, the Mn^{4+}/Mn^{3+} ratio decreases and larger Ti^{4+} or Cu^{2+} ions compress the neighboring Mn–O bonds, which results in the change of Mn–O–Mn bonds and the weakening of the double-exchange interaction [23].

4. Conclusions

In summary, the substitution of Ti or Cu doping on B site for Mn increases the infrared emissivity of lanthanum manganites, due to the infrared absorption in the 8–14 μm waveband. Decreasing transition probability indicated by ESR results leads to the decrease of emissivity with increasing doping level. The ε_N of B site doped lanthanum manganites changes slightly in the temperature range of 293–373 K, owing to the weakening of the double-exchange interaction between Mn^{3+} and Mn^{4+}.

Acknowledgements

We are thankful for the financial support provided by the National Natural Science Foundation of China (grant 90505008) and Weaponry Equipment Pre-research Foundation of China.

References

[1] S. Jin, T.H. Tiefel, M. McCormack, R.A. Fastnacht, R. Ramesh, L.H. Chen, Science 264 (1994) 413–415.
[2] Y. Tokura, N. Nagaosa, Science 288 (2000) 462–468.
[3] K. Mydeen, S. Arumugam, D. Prabhakaran, R.C. Yu, C.Q. Jin, J. Alloys Compd. 468 (2009) 280–284.
[4] X. Zhu, H. Shen, Z. Tang, K. Tsukamoto, T. Yanagisawa, M. Okutomi, N. Higuchi, J. Alloys Compd. 488 (2009) 437–441.
[5] C. Zener, Phys. Rev 82 (1951) 403–405.
[6] P.W. Anderson, H. Hasegawa, Phys. Rev. 100 (1955) 675–681.
[7] A.J. Millis, P.B. Littlewood, B.I. Shraiman, Phys. Rev. Lett. 74 (1995) 5144–5147.
[8] H.Y. Hwang, S.W. Cheong, P.G. Radaelli, M. Marezio, B. Batlogg, Phys. Rev. Lett. 75 (1995) 914–917.
[9] K. Shimazaki, S. Tachikawa, A. Ohnishi, Y. Nagasaka, Int. J. Thermophys. 22 (2001) 1549–1561.
[10] X. Shen, G. Xu, C. Shao, C. Cheng, J. Alloys Compd. 474 (2009) 375–377.
[11] G. Tang, Y. Yu, W. Chen, Y. Cao, J. Alloys Compd. 461 (2008) 486–489.
[12] B. Aslibeiki, P. Kameli, H. Salamati, Solid State Commun. 149 (2009) 1274–1277.
[13] T.S. Zhao, W.X. Xianyu, B.H. Li, Z.N. Qian, J. Alloys Compd. 459 (2008) 29–34.
[14] N. Kallel, N. Ihzaz, S. Kallel, A. Hagaza, M. Oumezzine, J. Magn. Magn. Mater. 321 (2009) 2285–2289.
[15] C. Castellano, M. Ferretti, A. Martinelli, M.R. Cimberle, J. Alloys Compd. 478 (2009) 479–483.
[16] P.T. Phong, N.V. Khiem, N.V. Dai, D.H. Manh, L.V. Hong, N.X. Phuc, J. Alloys Compd. 484 (2009) 12–16.
[17] P. Kameli, H. Salamati, A. Heidarian, H. Bahrami, J. Non-Cryst. Solids 355 (2009) 917–921.
[18] C. Xiong, H. Hu, Y. Xiong, Z. Zhang, H. Pi, X. Wu, L. Li, F. Wei, C. Zheng, J. Alloys Compd. 479 (2009) 357–362.
[19] M. El-Hagary, Y.A. Shoker, S. Mohammad, A.M. Moustafa, A. Abd El-Aal, H. Michor, M. Reissner, G. Hilscher, A.A. Ramadan, J. Alloys Compd. 468 (2009) 47–53.
[20] T. Arima, Y. Tokura, J. Phys. Soc. Japan 64 (1995) 2488–2491.
[21] K.H. Kim, J.Y. Gu, H.S. Choi, G.W. Park, T.W. Noh, Phys. Rev. Lett. 77 (1996) 1877–1880.
[22] K.Y. Wang, W.H. Song, J.M. Dai, S.L. Ye, S.G. Wang, J. Fang, J.L. Chen, B.J. Gao, J.J. Du, Y.P. Sun, J. Appl. Phys. 90 (2001) 6263–6267.
[23] A. Maignan, C. Martin, G. Van Tendeloo, M. Hervieu, B. Raveau, Phys. Rev. B 60 (1999) 15214–15219.